IEEE Access
Multidisciplinary ⋮ Rapid Review ⋮ Open Access Journal

Received June 26, 2021, accepted July 13, 2021, date of publication July 16, 2021, date of current version July 26, 2021.

Digital Object Identifier 10.1109/ACCESS.2021.3097742

Self-Adaptive Synergistic Optimization for Parameters Extraction of Synchronous Reluctance Machine Nonlinear Magnetic Model

YUANZHE ZHAO[1,2,3,4], LINJIE REN[1,2,3,4], GUOBIN LIN[4], ZHIMING LIAO[4], AND SIMING LIU[1,2,3,4]

[1]Key Laboratory of Road and Traffic Engineering of the State Ministry of Education, Shanghai 201804, China
[2]Key Laboratory of Rail Infrastructure Durability and System Safety, Tongji University, Shanghai 201804, China
[3]College of Transportation Engineering, Tongji University, Shanghai 201804, China
[4]National Maglev Transportation Engineering Research and Development Center, Tongji University, Shanghai 201804, China

Corresponding authors: Linjie Ren (org0000h@tongji.edu.cn) and Zhiming Liao (liaozhiming@tongji.edu.cn)

This work was supported in part by the Project of Science and Technology Commission Shanghai Municipality under Grant 17511102302, and in part by the National Key Technology Research and Development Program of China under Grant 2016YFB1200601.

ABSTRACT For mechanism analysis and high-performance control of synchronous reluctance machine (SynRM), accurate and reliable parameter identification of nonlinear magnetic model is always required. However, the accuracy and robustness of traditional heuristic algorithms are restricted by incomplete individual performance evaluation and single population evolution mechanism. In this paper, we propose a self-adaptive synergistic optimization (SSO) algorithm for extracting the parameters of the model. A novel synergistic-performance evaluation is first established to classify candidates automatically. Then, a self-organized mechanism is proposed to select optimal evolution strategies designed for classified candidate solutions. Around the current best candidate, the exploration is guaranteed in priority. Meanwhile, a self-adaptive mechanism is introduced to select other candidates to construct more promising evolutionary direction. Thus, achieving a good balance between exploration and exploitation. The parameter estimation performance of SSO algorithm is evaluated through standard datasets of SynRM magnetic model obtained by the finite element analysis. Comprehensive experiment results demonstrate the competitiveness and effectiveness of the proposed SSO algorithm compared with other algorithms, especially in terms of the accuracy and robustness. According to these superiorities, it can be concluded that the proposed algorithms are promising parameter identification methods for SynRM nonlinear magnetic model.

INDEX TERMS SynRM nonlinear magnetic model, parameters identification, optimization problem.

I. INTRODUCTION

In recent years, to cope with the energy consumption, cost, and over-dependence on rare earth elements rare-earth of AC motor, many efforts have been focused on the research of Synchronous Reluctance Motor (SynRM) [1]. Compared with induction motors (IM) and permanent magnet motors (PM), SynRM is the most promising alternative due to its high efficiency and structural robustness [2]. Hence, to control and optimize SynRM, it is critical to evaluate the actual nonlinear behaviors of magnetic circuit based on accurate model [3], [4]. In practice, the development of SynRM technology is restricted by the rationality and the parameters accuracy of the model. Therefore, a novel nonlinear magnetic model that satisfies the reciprocity conditions [5] and inherent properties is established. However, there are still some challenges in the parameter identification process of the proposed model. Such as inaccurate parameters and unstable results caused by the incomplete individual performance evaluation and single population evolution mechanism of traditional parameter identification algorithms.

The identification problem of magnetic model parameters can be transformed into an optimization problem, by solving the objective function between the proposed model and the flux linkage-current dataset. As reviewed in [6], least squares (LS) method have been used in the extraction of magnetic model parameters. Suffering from sensitivity to initial solution and dataset noise, the convergence of LS

The associate editor coordinating the review of this manuscript and approving it for publication was Xiaodong Liang.

results is unsatisfied and uncertain [7], [8]. As an alternative, metaheuristic algorithms are employed to identify the parameters of various motor model. In [9], a genetic algorithm (GA) was proposed for estimating the parameters of a saturation model using experimental test data under three working conditions. In [10], harmony search (HS) was utilized to identify parameters of a rational function-based inductance model. In [11], two improved particle swarm optimization algorithms (PSO) based strategy (dynamic PSO and chaos PSO algorithms) is proposed to estimate the parameters of induction motor model. The direct current, no-load and locked-rotor tests results are used for parameter estimation. Other algorithm variants such as self-adaptive differential evolution algorithm (SHDE) [12], dynamic encoding algorithm searches (DEAS) [13], fast parallel co-evolutionary PSO [14], GA assisted PSO algorithm [15] and dynamic PSO algorithm with learning strategies [16] are employed to identify the parameters of motor model. These metaheuristic algorithms have achieved certain results in parameter extraction of motor model. However, it is difficult to obtain the global optimal solution of the proposed model.

To address the above-mentioned problems of traditional metaheuristic algorithms in specific applications, various algorithms have been developed. In [17], [18] and [19], [20], Niche technologies based on crowding and fitness are adopted to evaluate the performance of candidate. In crowding based performance evaluation, the similar candidate solutions competition based on Euclidean distance is only allowed. The fitness evaluation-based algorithms often classify the candidates in the way of fitness sharing. Around the classified candidates, multiple optimal solutions are stably located in the niche [21], [22]. Although the above two methods are proved to be effective in evaluating the performance of the candidates to be selected, there are still problems in the comprehensive utilization of diversity and fitness information. Moreover, to cope with improper parameter configuration, a class of algorithms without special control parameters [23], [24] has attracted more and more attention. Recently, simple yet effective metaheuristics method named Rao algorithms [23] has been proposed by Rao for complex optimization problems. Due to the attractive characteristics, Rao algorithms have been widely applied to various real-world optimization problems such as photovoltaic cell parameter extraction [25]–[27], reinforced concrete retaining wall design [28], thermodynamic cycles system [29]. The distinguishing feature of Rao algorithms from other metaheuristic algorithms is the novel update mechanism of optimal solution search path. The interaction among individuals guided by fitness evaluation is the basis of exploration direction updating in search space. However, for existing metaheuristic algorithms, the fitness is not fully utilized in the process of optimal solution search path updating. Searching direction is only guided by fitness, ignoring the diversity information. The fitness and diversity performance of the candidate solution in population are not fully exploited, leading to the problems of stagnation and premature convergence.

The identification results of the existing parameter identification methods are restricted by the objective function and characteristics of the algorithm. On one hand, the parameter estimation of the pro-posed model is multimodal problem. There is always a certain degree of nonlinear noise in the flux linkage data obtained by the experimental method [30], [31] or the finite element analysis (FEA) [32]. The multimodality caused by nonlinear noise may make the traditional identification algorithm invalid. On the other hand, incomplete individual performance evaluation, limited evolutionary mechanism selection and improper specific control parameter configuration of many metaheuristic algorithms often results in premature termination. Hence, developing for a competitive metaheuristic algorithm to identify the proposed magnetic model parameters is still a challenging task.

In this paper, a self-adaptive synergistic optimization (SSO) algorithms is proposed to identify the parameters of SynRM magnetic model accurately and reliably. Specifically, a synergistic performance (SP) and fitness-based hybrid performance evaluation method is proposed. Based on the probability of the evaluation result, the candidates of the classification are chosen to construct different evolution directions using the proposed self-organizing evolution mechanism. In this way, the fitness and diversity contribution of the candidate solution to current population are comprehensively utilized. Besides, the mechanism for selecting update strategies for suboptimal and poor candidates is adaptive, without additional parameters are required. In this way, the candidates with better comprehensive performance are encouraged into new population, improving the quality of solution in each generation. Moreover, the evolutionary strategies involved in SSO algorithm are without specific control parameters, avoiding the risk of parameter mismatch. To evaluate the effectiveness of the proposed SSO algorithm, we compared them with other well-established algorithms on parameters identification problems of the SynRM magnetic model. Extensive experiments indicate that SSO algorithm exhibit superior performance in terms of accuracy and robustness.

To the best of our knowledge, no precedent that employs SSO algorithm to extract the parameters of the SynRM magnetic model has been published or reported publicly. The main contributions of this paper can be summarized as follows:

1) The SSO algorithm is first proposed to extract the parameters of SynRM magnetic model. Based on quantified SP, interactions among candidate solutions are introduced into the optimal search path updating to promote the related searching ability.
2) A simple and effective self-organizing mechanism is proposed to select promising evolution strategy for candidate self-adaptively. As a promising performance evaluation technology, the proposed mechanism can further improve the accuracy and reliability of parameter identification results. SP is defined to estimate fitness and diversity of candidates uniformly, which

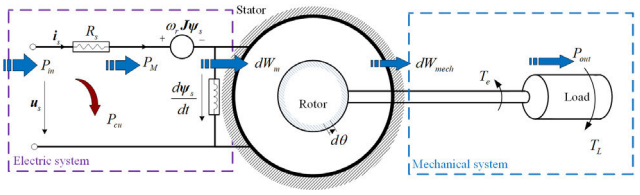

FIGURE 1. Electromechanical energy conversion process of SynRM.

can be a fundamental for quantifying balance between exploration and exploitation.

3) The effectiveness of SSO is demonstrated through comprehensive experiment for SynRM magnetic model parameter extraction.

The rest of this paper is structured in the following manner. Section II presents SynRM magnetic model, and the problem formulation. Section III provides the proposed SSO in detail. Validation results on SynRM magnetic model are shown and analyzed in Section IV. Finally, the conclusions are drawn in Section V.

II. MODELING OF SynRM

In this section, we propose a novel magnetic model of SynRM, and problem formulation are proposed. We focus on the model in $d-q$ reference frame (the d-axis align to the direction of maximum permeance) synchronous to the rotor. Besides, the magnetic energy change caused by the iron loss change is very small compared to that caused by the currents change. Therefore, the magnetic model is established under the following hypothesis: (1) The iron loss has been omitted. (2) The stator flux linkages are only dependent on stator currents. The details are shown as follows.

A. NONLINEAR MAGNETIC MODEL OF SynRM

Magnetic circuit nonlinearity can be characterized by the mapping among magnetic linkages and stator currents [4]. For modeling of magnetic model, the energy conversion mechanism determines the nonlinearity. As shown in Fig.1, SynRM is a typical singly excited electromechanical energy conversion device. It can be observed that the electrical and the mechanical systems are coupled by the magnetic energy (W_m) transformation. Under the assumption of conservative fields, the energy balance can be described as

$$\boldsymbol{i}_s^T \boldsymbol{u}_s = R_s \|\boldsymbol{i}_s\|^2 + \frac{dW_m}{dt} + T_e\omega_m \tag{1}$$

where $\boldsymbol{i}_s = (i_d, i_q)^{\mathrm{T}}, \boldsymbol{u}_s = (u_d, u_q)^{\mathrm{T}}, R_s, T_e, W_m, \omega_m$ are stator currents, stator voltages, stator winding resistance, electromagnetic torque, magnetic energy and mechanical velocity of the motor, respectively.

The energy conversion in coupling field is mediated by the change of magnetic energy. For convenience, the variation of magnetic energy can be expressed equivalently by the co-magnetic energy (W_c) [33]

$$\frac{dW_c}{dt} = \psi_d(i_d, i_q)\frac{di_d}{dt} + \psi_q(i_d, i_q)\frac{di_q}{dt} \tag{2}$$

where $\psi_d\ (i_d, i_q)$, $\psi_q\ (i_d, i_q)$ denotes nonlinear flux linkages respect to d-and q-axis, respectively. The flux linkages on d-and q-axis interact through a common magnetic circuit, resulting in redistribution of the flux linkage. This nonlinear behavior of the rotor magnetic circuit is called self-saturation and cross-saturation [6]. Under the assumption of conservative field, the cross-saturation process satisfies the conservation of energy. Therefore, the reciprocity condition [5] of can be obtained as

$$\frac{\partial\psi_d(i_d, i_q)}{\partial i_q} = \frac{\partial\psi_q(i_d, i_q)}{\partial i_d} \tag{3}$$

Combining (2) and (3), the modeling constraints of the flux linkage considering cross saturation are

$$\begin{cases} \psi_d(i_d, i_q) = \psi_d(i_d) - \dfrac{\partial\Delta W_c}{\partial i_d} \\ \psi_q(i_d, i_q) = \psi_q(i_q) - \dfrac{\partial\Delta W_c}{\partial i_q} \end{cases} \tag{4}$$

where $\psi_d(i_d)$, $\psi_q(i_d)$ are the flux linkages under the effect of self-saturation alone. ΔW_c represents the conversion of magnetic co-energy between d-and q-axis [4]. Under the restrictions (4) and (3), the flux linkage model based on the Gaussian's function is established as

$$\begin{cases} \psi_d(i_d, i_q) = \alpha_d(2 - e^{-\gamma_d i_d} - e^{-\gamma_{d1} i_d^2}) + \beta_d i_d \\ \qquad - k\left(2ai_d e^{-ai_d^2}\right)\left(bi_q^2 - i_q e^{-ci_q} + \kappa i_q - \dfrac{1}{c}e^{-ci_q}\right) \\ \psi_q(i_d, i_q) = \alpha_q(2 - e^{-\gamma_q i_q} - e^{-\gamma_{q1} i_q^2}) + \beta_q i_q \\ \qquad - k\left(1 - e^{-ai_d^2}\right)\left(2bi_q + ci_q e^{-ci_q} + \kappa\right) \end{cases} \tag{5}$$

where $\{\alpha, \gamma, \beta\}$ are non-negative self-saturation coefficients for the d-, and q-axis, and $\{k, \mathrm{a}, b, c, \kappa\}$ are cross-saturation coefficients. The subscripts d and q represent d-axis and q-axis. Based on (3), (4) and (5), the reciprocity condition and ΔW_c are expressed as

$$\begin{aligned} \frac{\partial\psi_d(i_d, i_q)}{\partial i_q} &= \frac{\partial\psi_q(i_d, i_q)}{\partial i_d} \\ &= -k\left(2ai_d e^{-ai_d^2}\right)\left(2bi_q + ci_q e^{-ci_q} + \kappa\right) \end{aligned} \tag{6}$$

$$\Delta W_c = -k\left(e^{-ai_d^2} - 1\right)\left(bi_q^2 - i_q e^{-ci_q} + \kappa i_q - e^{-ci_q}\right) \tag{7}$$

Thus, the analytical expressions of apparent inductances [3] can be obtained as

$$\begin{cases} L_d^{ai}(i_d, i_q) = \dfrac{\alpha_d(2 - e^{-\gamma_d i_d} - e^{-\gamma_{d1} i_d^2})}{i_d} + \beta_d \\ \qquad - k\left(2ae^{-ai_d^2}\right)\left(bi_q^2 - i_q e^{-ci_q} + \kappa i_q - \dfrac{1}{c}e^{-ci_q}\right) \\ L_q^{ai}(i_d, i_q) = \dfrac{\alpha_q(2 - e^{-\gamma_q i_q} - e^{-\gamma_{q1} i_q^2})}{i_q} + \beta_q \\ \qquad - k\left(1 - e^{-ai_d^2}\right)\left(2b + ce^{-Vi_q} + \dfrac{\kappa}{i_q}\right) \end{cases} \tag{8}$$

B. PROBLEM FORMULATION

To extract model parameters effectively, parameter extraction needs to be transformed into optimization problem. The goal is to obtain the smallest difference between reference data and simulated data. The cross-saturation parameters shared by the d- and the q-axis model are the premise of the optimization problem. The algorithm should be able to identify the no-load characteristics, self-saturation and cross-saturation characteristics cooperatively. To this end, error functions for the kth flux linkages respect to d- and q-axis can be formulated as

$$\begin{cases} f_k^d(\psi_d^r, i_d^r, i_q^r, \mathbf{x}_d) = \alpha_d \left(2 - e^{-\gamma_d i_d^r} - e^{-\gamma_d (i_d^r)^2}\right) \\ + \beta_d i_d^r - k\left(2ai_d^r e^{-a(i_d^r)^2}\right) \\ \times \left(b\left(i_q^r\right)^2 - i_q^r e^{-c\left(i_q^r\right)^2} + \kappa i_q^r - \frac{1}{c} e^{-ci_q^r}\right) - \psi_d^r \\ \mathbf{x}_d = \{\alpha_d, \gamma_d, \beta_d, k, a, b, c, \kappa\} \end{cases} \tag{9}$$

$$\begin{cases} f_k^q(\psi_q^r, i_d^r, i_q^r, \mathbf{x}_q) = \alpha_q \left(2 - e^{-\gamma_q i_q^r} - e^{-\gamma_q \left(i_q^r\right)^2}\right) + \beta_q i_q^r \\ - k\left(1 - e^{-a(i_d^r)^2}\right)\left(2bi_q^r + ci_q^r e^{-ci_q^r} + \kappa\right) - \psi_q^r \\ \mathbf{x}_q = \left\{\alpha_q, \gamma_q, \beta_q, k, a, b, c, \kappa\right\} \end{cases} \tag{10}$$

The objective functions defined by root mean square (RMSE) error can be obtained as follows:

$$\mathrm{RMSE}_d\left(\mathbf{x}_d\right) = \sqrt{\frac{1}{N}\sum_{k=1}^{N} f_d^k(\psi_d^r, i_d^r, i_q^r, \mathbf{x}_d)^2} \tag{11}$$

$$\mathrm{RMSE}_q\left(\mathbf{x}_q\right) = \sqrt{\frac{1}{N}\sum_{k=1}^{N} f_q^k(\psi_q^r, i_d^r, i_q^r, \mathbf{x}_q)^2} \tag{12}$$

where $\mathbf{x}$ is the decision variable, N is the sample number. $\mathbf{x}_d$, $\mathbf{x}_q$ are the obtained parameter vectors, where $\mathbf{x}_d = [\mathbf{x}_{d1}, \mathbf{x}_c]$, and $\mathbf{x}_q = [\mathbf{x}_{q1}, \mathbf{x}_c]$. $\mathbf{x}_{d1}$ and $\mathbf{x}_{q1}$ are the self-saturation parameters involved in $\mathbf{x}_d$ and $\mathbf{x}_q$, respectively, and $\mathbf{x}_c = [k, a, b, c, \kappa]$ is the common parameter sub-vector. N is the number of reference data.

III. SSO ALGORITHM

In this section, a detailed description of the proposed algorithm will be given. First, a new performance indicator named SP is proposed, which is unified quantification of the fitness and diversity contributions of the candidate solutions in current population. Then, we describe the self-organizing mechanism based on hybrid performance evaluation method. The core idea be-hind SSO is elucidated as follows.

A. HYBRID PERFORMANCE EVALUATION

In the evolution of population, exploitation and exploration are often in a trade-off relationship [34]. On one hand, the optimal search path update mechanism with excessive exploitation capacity may lead the more valuable search space is ignored. On the other hand, excessive exploration can easily produce low-quality solutions that do not contribute much to evolution. Hence, it is reasonable to find the part of the high-quality solution space that may be ignored, under the premise of guaranteeing the exploitation ability. From the perspective of the candidate solution, its performance is affected from two dimensions, fitness associated with exploitation and diversity related to exploration. It is unreasonable to guide the exploration of more promising solution spaces with adaptive evaluation alone. Inspired by [35], [36], fitness and diversity can be calculated by the objective function and the distance between the individual and the surrounding individual, respectively. However, it is impossible to evaluate the overall performance of the corresponding solution through a simple comparison, due to the different properties of the two functions. In addition, even if a comprehensive evaluation method based on these two functions can be found, to quantify the contribution of candidate solutions to the population is still an issue. Here, a probability-based synergistic performance (SP) for the k^{th} candidate solution $\mathbf{x}_k$ is defined as

$$P_s\left(\mathbf{x}_k, NP\right) = P_d\left(\mathbf{x}_k, NP\right) \cdot c_{k,s} + P_f\left(\mathbf{x}_k, NP\right) \cdot \left(1 - c_{k,s}\right) \tag{13}$$

where, $P_s(\mathbf{x}_k, NP)$, $P_f(\mathbf{x}_k, NP)$, $P_d(\mathbf{x}_k, NP)$, represent the SP, fitness performance (FP) and diversity performance (DP) for the candidate, respectively. $c_{k,s}$ is a random number in the range [0, 1], denoting synergistic coefficient (SC). The overall performance of the candidate in the current population is evaluated by SP. FP, DP represent the fitness and diversity contributions of the candidate in the current population, respectively.

The evolutionary process preference for exploration and exploitation maintenance can be quantified by SC, which also decided the proportion of FP and DP in SP evaluation. With the increase of SC, the preference for diversity increases in SP. On the contrary, the preference for fitness increases in SP. Particularly, when $c_{k,s} = 0$ or $c_{k,s} = 1$, SP degrade into FP or DP. In this situation, SP only evaluates the performance of the candidate from the perspective of fitness or diversity contribution. If SP is used as feedback, the performance of the candidate is only affected by exploitation or exploration preference of evolution. As the basis of SP construction, the quantification process of FP and DP is as follows.

The objective function $f(\mathbf{x}_k)$ is selected as the fitness function $f_{\text{fitness}}(\mathbf{x}_k)$ for each candidate solution.

$$f_{\text{fitness}}\left(\boldsymbol{x}_k\right) = f\left(\boldsymbol{x}_k\right) \tag{14}$$

Then the candidates are sorted in ascending order of fitness in the population, and probability based on ranking is used to reflect the fitness performance. The ranking and FP of $\mathbf{x}_k$ are presented in (15) and (16), respectively.

$$R_{\text{fitness}}\left(\boldsymbol{x}_k, N\right) = NP + 1 - i_k, \quad i_k = 1, 2, \ldots, NP \tag{15}$$

$$P_{k,f}\left(\boldsymbol{x}_k, NP\right) = \left(\frac{R_{\text{fitness}}\left(\boldsymbol{x}_k, NP\right)}{NP}\right)^2 \tag{16}$$

where i_k represents the fitness ranking of $\mathbf{x}_k$ in the population. The diversity function based on Euclidean distance [35]

between candidates is defined as

$$f_{\text{diversity}}(\boldsymbol{x}_k) = -\sum_{w=1}^{NP} \|\boldsymbol{x}_k - \boldsymbol{x}_w\|, \quad w = 1, 2, \ldots, NP \quad (17)$$

where $\|\boldsymbol{x}_k - \boldsymbol{x}_w\|$ represents the Euclidean distance between $\mathbf{x}_k$ and $\mathbf{x}_w$. The diversity ranking and DP are presented as follows.

$$R_{\text{diversity}}(\boldsymbol{x}_k, NP) = NP+1-j_k, \quad j_k = 1, 2, \ldots, NP \quad (18)$$

$$P_{k,d}(\boldsymbol{x}_k, NP) = \left(\frac{R_{\text{diversity}}(\boldsymbol{x}_k, NP)}{NP}\right)^2 \quad (19)$$

where j_k represents the fitness ranking of $\mathbf{x}_k$ in the population. (18) and (19) indicate that better performance corresponds to larger probability. The overall contribution of the candidates to the population is quantified by the random combination of the probabilities through SP. As a result, SP have advantage of theory-driven.

With the introduction of SP, the best and worst candidate solutions need to be redefined, as well as the selection process of high-quality candidate solutions. On one hand, the best and worst candidate solutions ($\mathbf{x}^s_{best}$ and $\mathbf{x}^s_{worst}$) no longer rely solely on fitness evaluation. Instead, they are obtained based on the largest or smallest SP in the current population. On the other hand, the evaluation of the merits of the candidates is not only related to their own fitness and diversity, but also related to the current population. In other words, if the FP and DP of the candidates have not changed in the previous search direction update, they will be recalculated before the search direction update. Then, the candidate with a larger P_s is selected in the comparison. In particularly, if the SP comparison results are equal, the candidate with a larger P_d wins. If P_d is still the same, the candidate with larger P_f wins. If all three P_s, P_d and P_f values are the same, the first candidate is chosen. Comparing SP of two candidate solutions is presented in Algorithm 1. If $\mathbf{x}^s_{best}$, $\mathbf{x}^s_{worst}$ and the chosen candidate are used as evolutionary guidance, evolutionary preferences will be affected by the inherent randomness of their SP. This random effect is automatic and does not require additional control parameters, hence the update direction of the candidate solution is expected to be guided into new search regions.

Algorithm 1 The Synergistic Performance Comparison Method

```
if P_s(x_k, NP) ≠ P_s(x_l, NP) then
  if P_s(x_k, NP) > P_s(x_l, NP) then
    return x_k
  else
    return x_l
  end if
else
  if P_d(x_k, NP) ≠ P_f(x_l, NP) then
    if P_d(x_k, NP) > P_f(x_l, NP) then
      return x_k
    else
      return x_l
    end if
  else
    if P_f(x_k, NP) ≠ P_f(x_l, NP) then
      if P_f(x_k, NP) > P_f(x_l, NP) then
        return x_k
      else
      return x_l
      end if
    else
      return x_k
    endif
  end if
end if
```

B. SELF-ORGANIZATION MECHANISM BASED ON HYBRID PERFORMANCE EVALUATION

Based on the probability of the hybrid performance evaluation of SP and fitness, the candidates are classified into three types: optimal, suboptimal and inferior. Then, the corresponding update strategy will be self-adaptively selected for each candidate to enhance the evolutionary ability of the population. For the optimal candidate with the largest contribution to fitness, the update strategy with emphasis on exploration capability will be assigned. For the other candidates, the self-adaptive mechanism based on SP are employed to select relevant evolutionary strategies. The candidate with larger SP were identified as suboptimal, the update strategy with more balanced exploration and exploitation will be allocated. For inferior candidate with smaller SP, the update strategy emphasis on exploitation will be assigned to converge toward the promising region located by better candidate. In view of this, the Self-organization mechanism can be described in Algorithm 2.

It can be observed that the evolutionary preferences can be quantified by SP, and the evolution process is also guided by SP. By using SP as feedback, the balancing between exploration ability and exploitation ability will be achieved reasonably.

The ultimate-goal of the self-organization mechanism is to locate the global optimal solution. Hence, the exploration strategy is committed to improve diversity and avoid local optimal. Therefore, based on the evaluation result of fitness contribution, the better of the two randomly selected candidates is employed to construct the more promising search direction. To be specific, as presented in (20), update direction is approaching the better candidate and away from the worse candidate.

$$x'_{fbest,v} = x_{fbest,v} + r_{1,fbset,v} \cdot \left(x^R_{fb,v} - x^R_{fw,v}\right) \quad (20)$$

where the superscript "R" represents the randomly selected candidate. $x_{fb,v}$, $x_{fw,v}$ represent the v^{th} variable for the better and worse candidate, respectively. $x'_{fbest,v}$ is the updated value

Algorithm 2 Pseudo Code of Self-Organization Mechanism

1: Evaluate *fitness* performance of each candidate using (20);
2: Identify the *fitness* performance optimal candidate $P_{fbest}(\mathbf{x}_{fbest}, NP)$;
3: **For** $k = 1$ to NP **do**
4: **if** $k = fbest$ **then**
5: Modify the best candidate using explorative strategy;
6: **else**
7: Randomly select $c_{k,s} \in \{0, 1\}$;
8: Evaluate Synergistic performance of each candidate using (17);
9: **if** $rand > P_s(\mathbf{x}_k, NP)$ **then**
10: Modify the suboptimal candidate using balancing strategy;
11: **else**
12: Modify the inferior candidate using exploitative strategy;
13: **end if**
14: **end if**
15: **end For**

of $x'_{k,v}$. $r_{1,fbest,v}$ is random numbers for the v^{th} variable in the range [0, 1].

As mentioned above, the update strategies corresponding to the suboptimal and inferior candidate are self-adaptively selected. The purpose is improving the exploitation ability while ensuring the diversity. Through probability-based SP quantification, diversity information and adaptability information are used as feedback to induce the evolution direction of the population. Specifically, candidates with better SP tend to maintain a balance between exploration and exploitation. As shown in (21), the modified update strategy in [23] is employed in this study.

$$x'_{k,v} = x_{k,v} + r_{1,k,v}\left(x^s_{best,v} - x^s_{worst,v}\right) + r_{2,k,v}\left(\left|x^s_{k,v} \text{ or } x^s_{l,v}\right| - \left|x^s_{l,v} \text{ or } x^s_{k,v}\right|\right) \quad (21)$$

where the superscript "s" represents the candidate for quantitative selection based on SP. $x_{best,v}, x_{worst,v}$ represent the v^{th} variable for the best and worst candidate, respectively. $x'_{k,v}$ is the updated value of $x_{k,v}$. $r_{1,k,v}$ and $r_{2,k,v}$ are the two random numbers for the v^{th} variable in the range [0, 1].

Moreover, devote to improving exploitation ability, as shown in (22), the modified update strategy of in [23] is employed. To realize the refined search around the inferior candidate. Only the candidates with the largest and smallest SP in the current population are selected to construct a new search direction. The search direction is still close to the best candidate solution and away from the worst candidate solution.

$$x'_{k,v} = x_{k,v} + r_{1,k,v}\left(x^s_{best,v} - x^s_{worst,v}\right) \quad (22)$$

Different from the original RAO-3 and RAO-1, the selected examples in the update strategy (21) and (22) are all

Algorithm 3 Pseudo Code of SSO Algorithm

1: Initialize population size *(NP)* and maximum number of function evaluations *(Max_FES)*;
2: Generate the initial population randomly, evaluate the objective function value of each individual;
3: $FES = NP$;
4: **While** $FES < Max\_FES$ **do**
5: Compute *fitness* performance P_f of each individual $\boldsymbol{x}_k$;
6: Compute *diversity* performance P_d of each individual $\boldsymbol{x}_k$;
7: Get *fitness best* individual $\mathbf{x}_{fbest}$ and fitness *worst* individual $\boldsymbol{x}_{fworst}$;
8: **For** $k = 1$ to NP **do**
9: **if** $k = fbest$ **then**
10: Modify the best solution by using (20);
11: **else**
12: Randomly select $c_{k,s} \in \{0, 1\}$;
13: Compute P_s each individual according to (13);
14: Get P_s *best* individual $\mathbf{x}^s_{best}$, and P_s *wrost* individual $\mathbf{x}^s_{worst}$;
17: Select $\boldsymbol{x}_{l1}, \boldsymbol{x}_{l2}$ from population randomly $(l1 \neq l2)$;
18: P_s comparison of $\boldsymbol{x}_{l1}, \boldsymbol{x}_{l2}$ by using **Algorithm 1**;
19: **if** $rand > P_s(k)$
19: Modify candidate solution by using (21);
19: **else**
Modify candidate solution by using (22);
end if
20: **end if**
21: Compute P_f of the updated individual $\boldsymbol{x}'_k$;
22: $FES = FES + 1$:
23: Accept the new solution if it is better than the old one;
24: **end for**
25: **End while**

calculated according to Algorithm 1. Whether the original update strategy or modified, the evolution of the population is critically affected by the best candidate solution, since other candidates are attracted to the region where it is located. Specifically, the original update strategies rely more on fitness when the search direction is updated, meanwhile the powerful exploitation ability has been achieved. For modified, due to the automatic intervention of the search direction, the stagnation and premature convergence in the evolution process are avoided. Consequently, a better balance exploration and exploitation can be achieved. Obviously, no additional parameters are introduced.

C. FRAMEWORK OF SSO

According to the mentioned above, Algorithm 3 gives the pseudo code of SSO algorithm and Fig. 2 provides the flow chart. The structure of the self-organization mechanism is

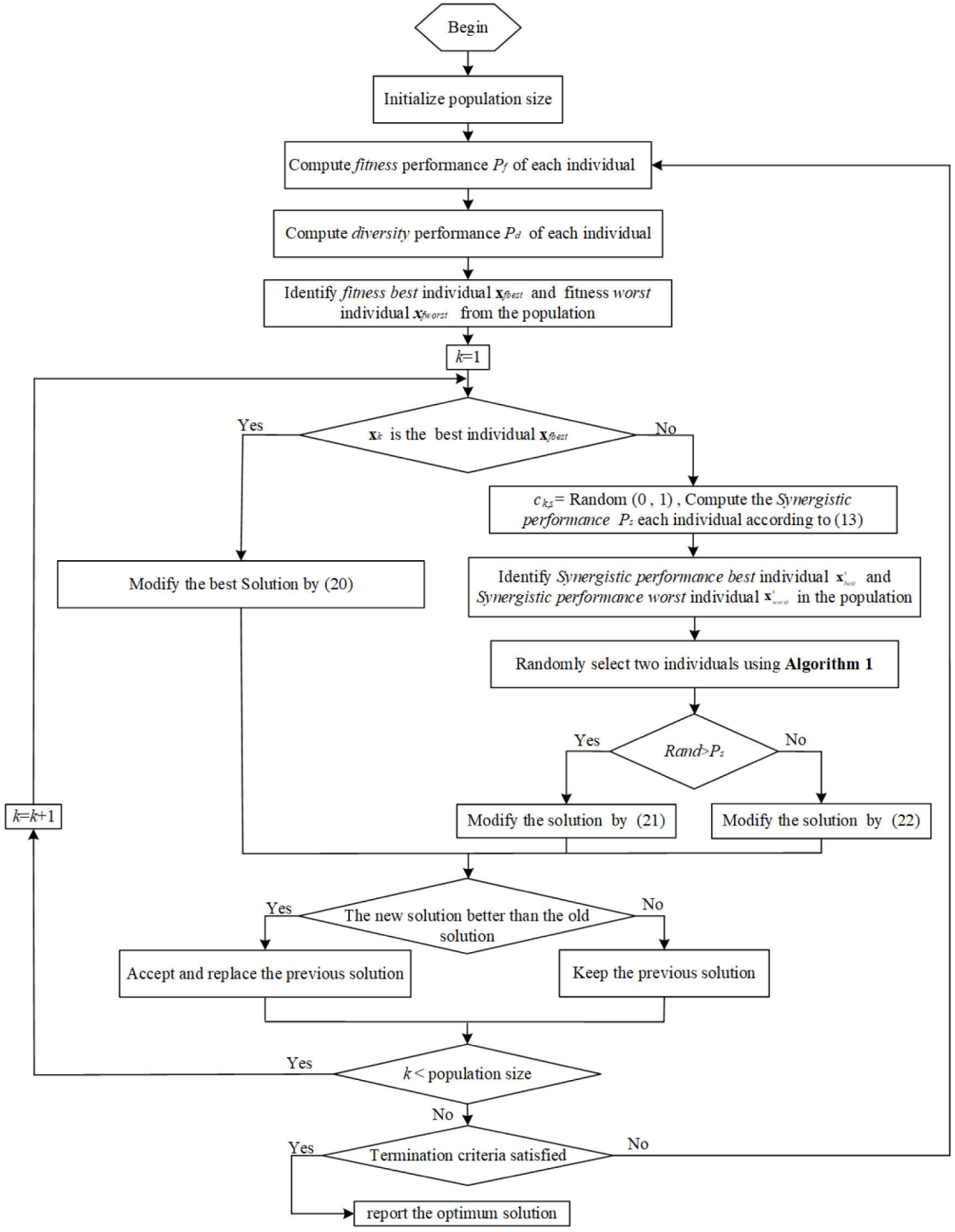

FIGURE 2. The flow diagram of SSO.

simple and clear, without special control parameters. No additional parameters need to be trained. During the operation of the algorithm, evolutionary preferences may be dynamically balanced, which is equivalent to the convergence strength being automatically managed.

As shown in Fig. 2, different strategies are employed to modify the FP optimal candidate and other candidates, which is equivalent to classifying the candidates in the current population. Considering that there are other optimal candidates nearby, a relatively conservative modification strategy is adopted to search the surrounding region. In this way, the powerful search capability of the original Rao algorithms can be inherited. On the contrary, for the other candidates, more radical modification strategies are employed to

improve population diversity as well as exploration capabilities. To this end, the performance of SSO algorithm may be superior to other algorithms.

In terms of the computational complexity, the proposed SSO algorithm have additional complexity from the SP quantification process compared with the original Rao algorithms, (i.e., diversity measure, population sorting and probability computation). Owing to the symmetric property of the distance measure, the complexity of diversity measure is $O(D.NP.(NP-2)/2)$, the complexity of population sorting is $O(3.NP.\log(NP)/2)$, and $O(3.NP/2)$ is consumed to calculate probability. Since the complexity of each original RAO algorithm is $O(G_{\max}.NP.D)$, where $G_{\max}$ is the maximal number of generations, the overall complexity of each SSO is $O(G_{\max}.NP.((D.NP+3.\log(NP)+3)/2))$. In general, the population size NP is set to be proportional to the problem dimension D. Thus, the overall complexity of SSO is $O(G_{\max}.NP.NP.D/2)$. Notes that the complexity of SSO is much lower than $O(G_{\max}.NP.NP.D/2)$. The distance measure is performed only when at least one individual of every pair is changed at current generation. Besides, compared with costly evaluation of the functions, the additional distance measurement cost can be ignored.

IV. VERIFICATION COMBINED WITH FEA

To verify the effectiveness of the proposed SSO algorithm, it was first employed to the parameter extraction problem of the SynRM nonlinear magnetic model. The flux linkages-stator currents data mentioned in section III are selected as the benchmark data. These data are obtained from the results of full-range FEA on the SynRM prototype, in which the stator currents interval is 1 A. Firstly, the comparisons are conducted on the best results represented by the RMSE values to illustrate the accuracy of each algorithm. And then, the robustness, effectiveness and parameter influences are analyzed and presented to evaluate comprehensive performance of each algorithm. The analysis software used in this paper is MATLAB.

A. PRELIMINARIES

FEA for the designed 2 kW prototype SynRM has been conducted. The design parameters of the prototype are summarized in Table 1. The operating condition data at special points are adopted as the reference for parameter identification in traditional method. Another purpose of implementing FEA on SynRM is to obtain a full range of operating characteristic data, which is used in subsequent parameter identification algorithms.

Aim to visualize the cross-saturation and the self-saturation phenomena more conveniently, the flux linkages based on FEA results are depicted in the first octant in Fig. 3. It can be seen from Fig. 3 that as the currents increase, the d- and q-axis flux linkages gradually show significant nonlinear behavior and are obviously affected by cross-magnetization, especially the q-axis flux linkage. The surface of ψ_d starts curved from i_d of 10 A, due to the self-saturation effect. The

TABLE 1. Parameters of the prototype.

Parameters	Values	Parameters	Values
Rated Power (kw)	2	Rated Voltage (V)	60
Rated Speed ($r\cdot min^{-1}$)	1500	Rated Current (A)	30
Rated Torque (N·m)	12.7	Number of pole pairs	2
Stator resistance (Ω)	0.3	Moment of inertia ($kg\cdot m^{-2}$)	0.025

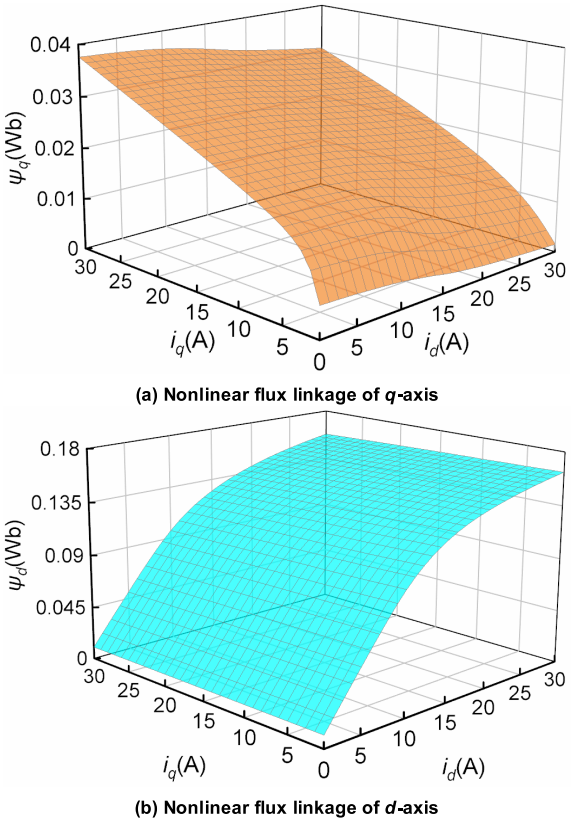

FIGURE 3. Nonlinear flux linkages of the prototype SynRM.

cross-saturation effect reflected in the decline of ψ_d along the direction of i_q increase. Similar nonlinear of ψ_q behaviors are also illustrated in Fig. 3. It can also be concluded that the q-axis current has a deeper effect on d- and q-axis flux linkages, whereas d- and q-axis flux linkage are mostly affected by the current in the corresponding axis

Fig. 3 shows that that the modeling principle of the nonlinear behaviors in magnetic circuit is reasonable. To extract the parameters of magnetic model, the objective function needs to be constructed by combining (5) and EFA results.

To evaluate the superior performance of the proposed SSO algorithm, comparative experiments are carried out with already well-established algorithms. These algorithms are the original Rao algorithms [23], Grey Wolf Optimization (GWO) algorithm [39], Ant Lion Optimization (ALO) algorithm [40], JAYA algorithm [24], biogeography-based learning particle swarm algorithm (BLPSO) [7], comprehensive learning particle swarm optimizer (CLPSO) [41],

differential evolution with biogeography-based optimization (DE/BBO) [42] and DE/BBO with covariance matrix-based migration (CMM-DE/BBO) [43]. These ten algorithms were selected due to their superior performance in parameter identification. The superiority of GWO and ALO over other algorithms such as DE, and PSO has been demonstrated in [39] and [40]. Thus, two excellent variants of DE and PSO are chosen for comparison.

As shown in (5), the proposed SynRM magnetic model is a dual function model with common parameters. Due to the standard datasets of the d-axis and q-axis models are relatively independent, a two-stage experiment is designed and implemented to identify parameters by using the algorithms involved. The algorithms are first employed to identify the parameters of the q-axis model, since the reference data corresponding to the q-axis model are smaller. Then, the common parameters obtained are used for the extraction of d-axis self-saturation parameters. The purpose of the two-stage experimental setup is not only to ensure that the parameters of the d-and q-axis models are accurately identified, but also to ensure that the reciprocity conditions are not violated.

For the sake of fairness, the parameter configuration of the experiment is the same for different algorithms. The parameter range is fixed to ensure the same search space. The same maximum number of function evaluations (*Max_FES*) for all algorithms is set to 30000 in each run. To reduce the statistical error as far as possible, each algorithm is independently conducted 30 times on the problem. Besides, the population size in different experimental stages is set to different values. The influence of population size on the performance of the proposed SSO algorithm will be discussed in subsection D. The parameter configuration of all comparison algorithms is given in Table 2.

TABLE 2. Parameter configuration of comparison algorithms.

Model	Population size	Run times	*Max_FES*	Parameters range	
				Lower	Upper
q-axis flux linkage model	NP=20	30	30000	0	2
d-axis flux zlinkage model	NP=30	30	30000	0	2

B. RESULTS ON Q-AXIS FLUX LINKAGE MODEL

For the q-axis flux linkage model, 11 different algorithms are independently implemented 30 times to obtain its self-saturation and cross-saturation parameters. Due to the exact values of the model parameters are unknown, RMSEq is taken as the standard of accuracy evaluation. The comparison of the best parameter values and the best RMSE among the 30 identification results of different algorithms is given in Table 3. Among them, the best RMSEq are marked in bold. It can be seen from Table 3 that SSO algorithm achieve better accuracy than other algorithms, and SSO algorithm provide

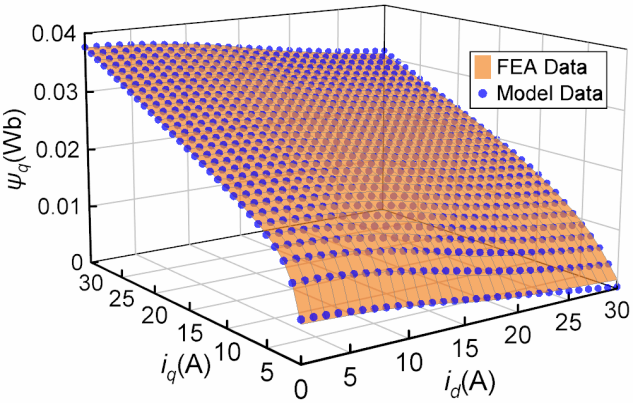

FIGURE 4. Comparisons between FEA data and estimated data obtained by SSO for q-axis flux linkage model.

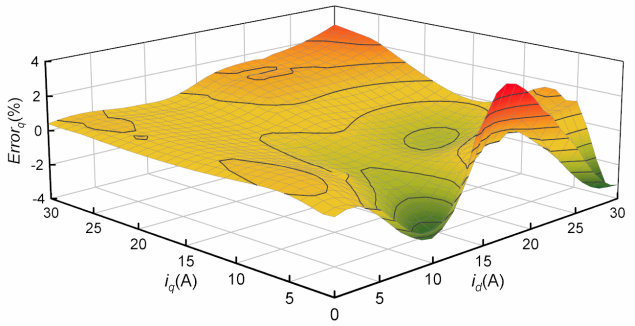

FIGURE 5. Mismatch of q-axis flux linkage, estimated value vs FEA value.

the best RMSEq value (2.2243E-04). The second-best result (2.3034E-04) is provided by Rao-1. Although the RMSEq of some algorithms is very close to the results obtained by SSO algorithm, a smaller RMSEq is conducive to determine the true parameters of the model.

To further illustrate the excellent results of the identification results, the q-axis flux linkage map is reconstructed using the best results of SSO algorithm. Fig.4 (a) shows the estimated value of q-axis flux linkage and FEA value in the full range of working conditions. Obviously, the estimated value of q-axis flux linkage in the entire current range is highly consistent with its FEA value.

The absolute error rate (AER) between the estimated value and the FEA value is shown in Fig.5. Except for the very few points on the edge of the model where the AER is close to 4%, the AER at other contrast points does not exceed 1%. A few large absolute errors cannot be attributed to the parameter identification algorithm, which is related to the modeling method and the calculation error of FEA at the model boundary. Due to the errors at special point are known, the model with the identified parameters can be successfully used in actual engineering.

To further evaluate the robustness of the proposed algorithms. Analysis based on RMSE statistics is implemented. The statistical results of the parameter identification of the dual function model by 11 algorithms that run 30 times

TABLE 3. Comparison among different algorithms on q-axis flux linkage model.

Algorithm	self-saturation coefficients				cross-saturation coefficients					RMSEq
	α_q	β_q	γ_q	γ_{q1}	k	W	V	V_1	κ_q	
SSO	**0.0072**	**1.0324**	**0.1233**	**7.8240E-04**	**0.0216**	**0.0020**	**0.0114**	**0.2633**	**0.0758**	**2.2243E-04**
GWO	0.0071	1.0610	0.1251	7.8437E-04	0.0198	0.0021	0.0112	0.2685	0.1083	2.3034E-04
ALO	0.0140	0.0014	0.3133	7.7888E-04	0.0197	0.0033	0.0109	0.2151	0.0041	6.9356E-04
BLPSO	0.0070	0.4307	0.4166	7.9459E-04	0.0180	0.0021	0.0121	0.2915	0.1393	2.9613E-04
CLPSO	0.0127	0.0218	0.6777	6.2413E-04	0.0105	1.1194	0.0049	0.4572	0.1498	0.0022
DE/BBO	0.0072	0.4329	0.3368	7.7735E-04	0.0212	0.0023	0.0450	0.2157	2.0000	2.6629E-04
CMM-DE/BBO	0.0070	0.8631	0.2983	7.9557E-04	0.0226	0.0020	0.01150	0.2808	0.0640	2.4377E-04
Rao-1	0.0071	1.0297	0.1238	7.8393E-04	0.0215	0.0020	0.0115	0.2633	0.0751	2.2443E-04
Rao-2	0.0079	0.2632	0.6453	7.0144E-04	0.0215	0.0020	0.0115	0.2633	0.0751	5.8524E-04
Rao-3	0.0072	1.6691	0.0597	7.6864E-04	0.0042	0.0016	0	2.0000	2.0000	7.0207E-04
JAYA	0.0141	0.4671	0	7.6524E-04	0.0050	0.0012	0.0072	0.9533	1.7820	6.9965E-04

TABLE 4. Statistical results of RMSE of different algorithms for q-axis model (30000 function evaluations).

Model	Population size	Algorithm	RMSE			
			B	M	W	SD
q-axis flux linkage model	NP=30	SSO	**2.2243E-04**	**2.8630E-04**	**6.4661E-04**	**1.1597E-04**
		GWO	2.3034E-04	0.0018	0.0050	0.0012
		ALO	6.9356E-04	0.0022	0.0049	0.0010
		BLPSO	2.9613E-04	4.8678E-04	8.5550E-04	1.3891E-04
		CLPSO	0.0022	0.0059	0.0420	0.0077
		DE/BBO	2.6629E-04	0.0012	0.0121	0.0024
		CMM-DE/BBO	2.4377E-04	7.4912E-04	0.0024	6.7630E-04
		Rao-1	2.2243E-04	0.0017	0.0238	0.0043
		Rao-2	5.8524E-04	0.0053	0.0238	0.0074
		Rao-3	7.0207E-04	0.0073	0.0238	0.0093
		JAYA	6.9965E-04	0.0031	0.0074	0.0016

independently are given in Table 4. The results of the algorithms involved are calculated according to the best RMSE (B), worst RMSE (W), average RMSE (M), and standard deviation RMSE (SD). The best result in the corresponding algorithm is indicated in bold.

In terms of average accuracy and robustness, it can be clearly observed from Table 4 that the overall performance of the proposed SSO algorithm is better than other algorithms. For q-axis flux linkage model, the best M (2.8630E-04) and best SD (1.1597E-04) are provided by the proposed SSO algorithm. Among other algorithms, the average accuracy and robustness of BLPSO and CMM-DE/BBO are also considerable, but neither BLPSO nor CMM-DE/BBO provides the best RMSEq. In addition, the distribution characteristics of the results of 30 independent runs of 11 algorithms are presented in Fig. 6 using box plots. The distribution range of the parameter identification results also demonstrates the superiority of the proposed SSO algorithm. The results distribution corresponding to the SSO algorithm is the most concentrated.

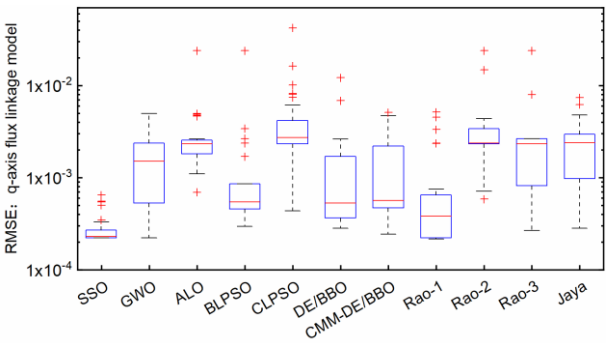

FIGURE 6. Best RMSE boxplot over 30 runs of different algorithms for q-axis flux linkage model.

C. RESULTS ON D-AXIS FLUX LINKAGE MODEL

As the second stage of SynRM magnetic model parameter identification, the extraction of the d-axis model parameters is similarly to the process mentioned in the previous subsection. The best cross-saturation coefficients are applied to the identification of the parameters of the model. Thus, there are only four parameters to be identified. The best estimated parameters and the best RMSEd of different algorithms are listed in Table 5. Clearly, the proposed SSO algorithm also provide the best RMSEd value (4.0815E-4) among all compared algorithms, and Rao-3 obtains the second best RMSEd value (4.0817E-04). The fit between the d-axis flux linkage map reconstructed by the estimated value and the FEA data is given in Fig. 7. As shown in Fig. 8, the overwhelming majority AER values are less than 1%, indicating that the high-accurately identified parameters are provided.

For d-axis flux linkage model, the robustness and stability analysis results of the SSO algorithm are shown in Table 6 and Fig. 9, respectively. Compared with other algorithms, SSO algorithm also shows the best performance.

TABLE 5. Comparison among different algorithms on d-axis flux linkage model.

Model	Population size	Algorithm	RMSE			
			B	M	W	SD
d-axis flux linkage model	*NP*=30	SSO	**4.0815E-04**	**4.0826E-04**	**4.0893E-04**	**2.1261E-07**
		GWO	4.0818E-04	0.0029	0.0232	0.0056
		ALO	4.2398E-04	0.0032	0.0180	0.0017
		BLPSO	5.2488E-04	0.0012	0.0020	4.2742E-04
		CLPSO	9.0099E-04	0.0036	0.0100	0.0018
		DE/BBO	4.5824E-04	0.0036	0.0079	0.0022
		CMM-DE/BBO	4.0818E-04	0.0021	0.0058	0.0016
		Rao-1	4.0866E-04	0.0010	0.0034	0.0014
		Rao-2	4.0821E-04	0.0028	0.0232	0.0041
		Rao-3	4.0817E-04	0.0023	0.0034	0.0012
		JAYA	4.0828E-04	0.0018	0.0036	0.0013

TABLE 6. Statistical results of RMSE of different algorithms for d-axis model (30000 function evaluations).

Algorithm	self-saturation coefficients				RMSE*d*
	α_d	β_d	γ_d	γ_{d1}	
SSO	**0.0615**	**0.1498**	**0.0100**	**0.0013**	**4.0815E-04**
GWO	0.0615	0.1498	0.0100	0.0013	4.0818E-04
ALO	0.0623	0.1484	0.0098	0.0013	4.2398E-04
BLPSO	0.0595	0.1491	0.0108	0.0015	5.2488E-04
CLPSO	0.0613	0.1665	0.0086	0.0014	9.0099E-04
DE/BBO	0.0602	0.1509	0.0104	0.0014	4.5824E-04
CMM-DE/BBO	0.0615	0.1498	0.0100	0.0013	4.0818E-04
Rao-1	0.0615	0.1500	0.00995	0.0013	4.0866E-04
Rao-2	0.0616	0.1497	0.0100	0.0013	4.0821E-04
Rao-3	0.0615	0.1498	0.0100	0.0013	4.0817E-04
JAYA	0.0619	0.1499	0.0099	0.0013	4.0828E-04

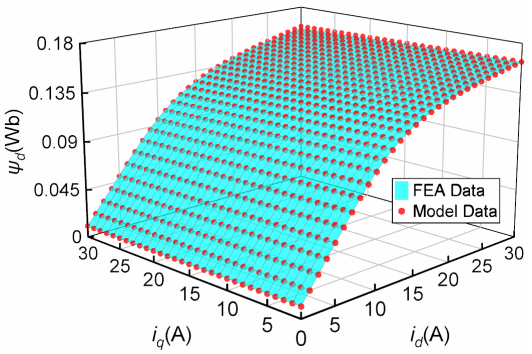

FIGURE 7. Comparisons between FEA data and estimated data obtained by SSO for *d*-axis flux linkage model.

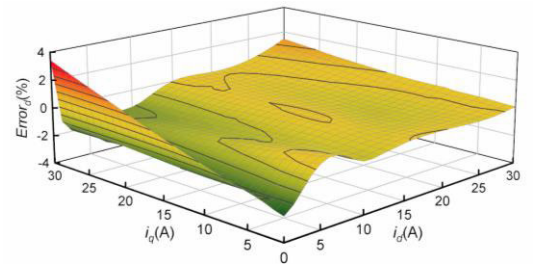

FIGURE 8. Mismatch of *d*-axis flux linkage, estimated value vs FEA value.

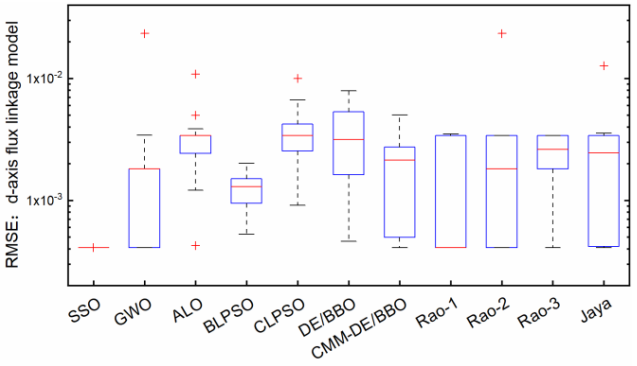

FIGURE 9. Best RMSE boxplot over 30 runs of different algorithms for *d*-axis flux linkage model.

D. RESULTS DISCUSSION

The comparison results demonstrate that the proposed SSO algorithm has better accuracy and reliability for solving the parameters identification problems of SynRM magnetic model, and its performance is competitive in contrast with all compared algorithms. The difference between the best RMSE*d* and the best RMSE*q* provided by the proposed SSO algorithm can be clearly observed. On one hand, although the accuracy of the experimental results in *q*-axis model is considerable, the algorithm error is inevitably introduced into *d*-axis model with the application of cross-saturation parameters. On the other hand, the energy loss of the rotor region corresponding to *d*-and *q*-axis is different. These losses are not reflected in the cross-saturation parameters under conservative field assumptions. This makes the influence of the loss contained in the standard datasets equivalent to a kind of noise, which is accumulated and introduced into the identification result of the *d*-axis self-saturation parameter. Fortunately, the magnitudes of the best RMSE*d* and the best RMSE*q* are equal, thus the superior accuracy and robustness of the proposed SSO algorithm can be explained in one aspect.

To verify the effectiveness of the proposed hybrid performance evaluation, comparative experiments for a variant of SSO algorithm are implemented in this subsection. The algorithms are obtained by modifying the evolution strategies and performance evaluation of the SSO algorithm. For the

TABLE 7. Statistical results of RMSE of different SSO algorithm for SynRM magnetic model (30000 function evaluations).

Model	Population size	Algorithm	RMSE			
			B	M	W	SD
q-axis flux linkage model	NP=30	SSO	**2.2243E-04**	**2.8630E-04**	**6.4661E-04**	**1.1597E-04**
		M-SSO	2.2243E-04	0.0097	0.2617	0.0476
d-axis flux linkage model	NP=30	SSO2	4.0815E-04	4.0826E-04	4.0893E-04	2.1261E-07
		M-SSO3	0.0111	0.0112	0.0113	6.6143E-05

TABLE 8. Statistical results of SSO algorithm with varying NP for SynRM magnetic model (30000 function evaluations).

Model	RMSE	Population size				
		NP=10	NP=20	NP=30	NP=40	NP=50
q-axis flux linkage model	B	2.2243E-04	2.2243E-04	**2.2243E-04**	4.4533E-04	7.7220E-04
	M	3..3406E-04	4.3331E-04	**2.8630E-04**	0.0011	0.0015
	W	0.0023	0.0022	**6.4661E-04**	0.0022	0.0024
	SD	3.9814E-04	3.7139E-04	**1.1597E-04**	4.4985E-04	4.6546E-04
d-axis flux linkage model	B	4.0815E-04	4.0815E-04	**4.0815E-04**	4.0827E-04	4.0883E-04
	M	6.2669E-04	4.1046E-04	**4.0826E-04**	5.0583E-04	9.1549E-04
	W	0.0056	4.7749E-04	**4.0893E-04**	0.0023	0.0058
	SD	9.6863E-04	1.2660 E -05	**2.1261E-07**	3.5001E-04	0.0012

mechanism of SSO algorithm, the interaction among candidate does not depend on SP (denoted as M-SSO). The self-organization mechanism is not induced by SP. Note that SP evolution strategies will degenerate to the original Rao-1 and Rao-3. The statistical results of the two variants are presented in Table 7. For each model, the values shown in bold in Table 7 indicate the comparatively better results of the respective algorithms. In terms of average accuracy and robustness, it can be clearly observed from Table 7 that the over-all performance of the proposed SSO algorithm is better than the variant. The obvious difference between the results of the SSO algorithm and the corresponding variant indicates that the hybrid performance evaluation-based self-organization mechanism is beneficial to optimize the original Rao-1 and Rao-3.

As mentioned previous, the proposed SSO algorithm are free from the algorithm-specific parameters, its performance is still affected by the population size. To this end, the experiments on SSO algorithm with different population sizes are implemented. The SSO algorithm with $NP = 10$, 20, 30, 40 and 50 is tested and compared, maintaining the *Max_FES* maintained at 30,000. Note that the experiment is still implemented in two stages. The statistical results of SSO algorithm with different population sizes are presented in Table 8. The comparison results show that the impact of population size on different algorithms at different experimental stages is consistent. From the perspective of the accuracy, too large population size is not conducive to obtaining the best and the average RMSE. From the perspective of robustness, too small or too large population size will worsen robustness. It can be clearly seen that due to the different dimensions of the problem, the optimal population size for different problems is also different. Hence, the most appropriate population size for parameter identification of d- and q-axis flux models is set to 30.

V. CONCLUSION

In this paper, we have proposed some novel SSO algorithm to accurately and steadily extract the parameters of the SynRM nonlinear magnetic model. In SSO algorithm, the hybrid performance evaluation is presented to uniformly evaluate the contribution of the fitness and diversity of candidate solutions. The algorithm aims to self-adaptively assign suitable update strategies for the candidates. Through the induction of self-organization mechanism based on performance probability, a good balance between exploration and exploitation can be achieved. In addition, the proposed SSO algorithms are simple enough in structure without additional parameters to be tuned, so as to be easily implemented. Experiment results show that SSO algorithm perform better in terms of accuracy and reliability when compared with other well-established algorithms. Obviously, the SSO algorithm are effective enough to solve the parameters identification problems of SynRM nonlinear magnetic model.

Moreover, through the verification of the proposed SynRM model parameter identification, it can be inferred that the proposed algorithm can be extended to the solution of the multi-parameter and multi-peak problem. On the basis of the research in this study, in view of the noise characteristics of the measured reference data, it is necessary to further study the evolution strategy of metaheuristic algorithm with higher robustness to further improve the accuracy of the SynRM magnetic model parameter identification.

REFERENCES

[1] W. T. Villet and M. J. Kamper, "Variable-gear EV reluctance synchronous motor drives—An evaluation of rotor structures for position-sensorless control," *IEEE Trans. Ind. Electron.*, vol. 61, no. 10, pp. 5732–5740, Oct. 2014.

[2] Z. Yang, F. Shang, I. P. Brown, and M. Krishnamurthy, "Comparative study of interior permanent magnet, induction, and switched reluctance motor drives for EV and HEV applications," *IEEE Trans. Transport. Electrific.*, vol. 1, no. 3, pp. 245–254, Oct. 2015.

[3] S. Wiedemann, S. Hall, R. M. Kennel, and M. Alakula, "Dynamic testing characterization of a synchronous reluctance machine," *IEEE Trans. Ind. Appl.*, vol. 54, no. 2, pp. 1370–1378, Mar. 2018.

[4] Z. Qu, T. Tuovinen, and M. Hinkkanen, "Inclusion of magnetic saturation in dynamic models of synchronous reluctance motors," in *Proc. ICEM*, Sep. 2012, pp. 994–1000.

[5] J. A. Melkebeek and J. L. Willems, "Reciprocity relations for the mutual inductances between orthogonal axis windings in saturated salient-pole machines," *IEEE Trans. Ind. Appl.*, vol. 26, no. 1, pp. 107–114, Jan./Feb. 1990.

[6] S. A. Odhano, P. Pescetto, H. A. A. Awan, M. Hinkkanen, G. Pellegrino, and R. Bojoi, "Parameter identification and self-commissioning in AC motor drives: A technology status review," *IEEE Trans. Power Electron.*, vol. 34, no. 4, pp. 3603–3614, Apr. 2019.

[7] Q. Niu, L. Zhang, and K. Li, "A biogeography-based optimization algorithm with mutation strategies for model parameter estimation of solar and fuel cells," *Energy Convers. Manag.*, vol. 86, pp. 1173–1185, Oct. 2014.

[8] K. Yu, X. Chen, X. Wang, and Z. Wang, "Parameters identification of photovoltaic models using self-adaptive teaching-learning-based optimization," *Energy Convers. Manage.*, vol. 145, pp. 233–246, Aug. 2017.

[9] A. Accetta, M. Cirrincione, M. Pucci, and A. Sferlazza, "A saturation model of the synchronous reluctance motor and its identification by genetic algorithms," in *Proc. IEEE Energy Convers. Congr. Expo.*, Sep. 2018, pp. 4460–4465.

[10] Y. Qiu, Q. Kang, L. Wang, and Q. Wu, "A parameter optimization method for dq axis inductance model of synchronous reluctance motors considering cross-coupling magnetic saturation," *Diangong Jishu Xuebao/Trans. China Electrotech. Soc.*, vol. 32, pp. 85–92, Feb. 2017.

[11] D. C. Huynh and M. W. Dunnigan, "Parameter estimation of an induction machine using advanced particle swarm optimization algorithms," *IET Electr. Power Appl.*, vol. 4, no. 9, pp. 748–760, Nov. 2010.

[12] C. Wang, Y. Liu, X. Liang, H. Guo, Y. Chen, and Y. Zhao, "Self-adaptive differential evolution algorithm with hybrid mutation operator for parameters identification of PMSM," *Soft Comput.*, vol. 22, no. 4, pp. 1263–1285, Feb. 2018.

[13] J.-W. Kim and S. W. Kim, "Parameter identification of induction motors using dynamic encoding algorithm for searches (DEAS)," *IEEE Trans. Energy Convers.*, vol. 20, no. 1, pp. 16–24, Mar. 2005.

[14] Z.-H. Liu, X.-H. Li, L.-H. Wu, S.-W. Zhou, and K. Liu, "GPU-accelerated parallel coevolutionary algorithm for parameters identification and temperature monitoring in permanent magnet synchronous machines," *IEEE Trans. Ind. Informat.*, vol. 11, no. 5, pp. 1220–1230, Oct. 2015.

[15] C.-F. Juang, "A hybrid of genetic algorithm and particle swarm optimization for recurrent network design," *IEEE Trans. Syst., Man, Cybern. B, Cybern.*, vol. 34, no. 2, pp. 997–1006, Apr. 2004.

[16] Z. H. Liu, H. L. Wei, Q. C. Zhong, and K. Liu, "Parameter estimation for VSI-fed PMSM based on a dynamic PSO with learning strategies," *IEEE Trans. Power Electron.*, vol. 32, no. 4, pp. 3154–3165, Apr. 2017.

[17] R. Thomsen, "Multimodal optimization using crowding-based differential evolution," in *Proc. IEEE Congr. Evol. Comput.*, Jun. 2004, pp. 1382–1389.

[18] M. Li, D. Lin, and J. Kou, "A hybrid niching PSO enhanced with recombination-replacement crowding strategy for multimodal function optimization," *Appl. Soft Comput.*, vol. 12, no. 3, pp. 975–987, 2012.

[19] P. S. Oliveto, D. Sudholt, and C. Zarges, "On the benefits and risks of using fitness sharing for multimodal optimisation," *Theor. Comput. Sci.*, vol. 773, pp. 53–70, Jun. 2019.

[20] C.-Y. Lin and W.-H. Wu, "Niche identification techniques in multimodal genetic search with sharing scheme," *Adv. Eng. Softw.*, vol. 33, nos. 11–12, pp. 779–791, Nov. 2002.

[21] X. Li, M. G. Epitropakis, K. Deb, and A. Engelbrecht, "Seeking multiple solutions: An updated survey on niching methods and their applications," *IEEE Trans. Evol. Comput.*, vol. 21, no. 4, pp. 518–538, Aug. 2017.

[22] J.-P. Li, M. E. Balazs, G. T. Parks, and P. J. Clarkson, "A species conserving genetic algorithm for multimodal function optimization," *Evol. Comput.*, vol. 10, no. 3, pp. 207–234, 2002.

[23] R. V. Rao, "Rao algorithms: Three metaphor-less simple algorithms for solving optimization problems," *Int. J. Ind. Eng. Comput.*, vol. 11, no. 1, pp. 107–130, 2020.

[24] R. V. Rao, "Jaya: A simple and new optimization algorithm for solving constrained and unconstrained optimization problems," *Int. J. Ind. Eng. Comput.*, vol. 7, no. 1, pp. 19–34, 2016.

[25] M. Premkumar, T. S. Babu, S. Umashankar, and R. Sowmya, "A new metaphor-less algorithms for the photovoltaic cell parameter estimation," *Optik*, vol. 208, Apr. 2020, Art. no. 164559.

[26] T. S. Babu, D. Yousri, and K. Balasubramanian, "Photovoltaic array reconfiguration system for maximizing the harvested power using population-based algorithms," *IEEE Access*, vol. 8, pp. 109608–109624, 2020.

[27] L. Wang, Z. Wang, H. Liang, and C. Huang, "Parameter estimation of photovoltaic cell model with Rao-1 algorithm," *Optik*, vol. 210, May 2020, Art. no. 163846.

[28] E. N. Kalemci and S. B. Ikizler, "Rao-3 algorithm for the weight optimization of reinforced concrete cantilever retaining wall," *Geomech. Eng.*, vol. 20, no. 6, pp. 527–536, Mar. 2020.

[29] R. V. Rao and H. S. Keesari, "Rao algorithms for multi-objective optimization of selected thermodynamic cycles," *Eng. With Comput.*, vol. 36, pp. 1–29, Mar. 2020.

[30] N. Bedetti, S. Calligaro, and R. Petrella, "Stand-still self-identification of flux characteristics for synchronous reluctance machines using novel saturation approximating function and multiple linear regression," *IEEE Trans. Ind. Appl.*, vol. 52, no. 4, pp. 3083–3092, Jul. 2016.

[31] L. Peretti, P. Sandulescu, and G. Zanuso, "Self-commissioning of flux linkage curves of synchronous reluctance machines in quasi-standstill condition," *IET Electr. Power Appl.*, vol. 9, no. 9, pp. 642–651, Nov. 2015.

[32] M. Gamba, G. Pellegrino, A. Cavagnino, Z. Gmyrek, and M. Lefik, "Impact of rotor end effects on FEM-based flux mapping of synchronous reluctance motors," *IEEE Trans. Ind. Appl.*, vol. 54, no. 5, pp. 4114–4122, Sep./Oct. 2018.

[33] D. Mingardi, M. Morandin, S. Bolognani, and N. Bianchi, "On the proprieties of the differential cross-saturation inductance in synchronous machines," *IEEE Trans. Ind. Appl.*, vol. 53, no. 2, pp. 991–1000, Mar. 2017.

[34] P. Guglielmi, M. Pastorelli, and A. Vagati, "Impact of cross-saturation in sensorless control of transverse-laminated synchronous reluctance motors," *IEEE Trans. Ind. Electron.*, vol. 53, no. 2, pp. 429–439, Apr. 2006.

[35] S. Chalermchaiarbha and W. Ongsakul, "Stochastic weight trade-off particle swarm optimization for nonconvex economic dispatch," *Energy Convers. Manage.*, vol. 70, pp. 66–75, Jun. 2013.

[36] J. Wang, J. Liao, Y. Zhou, and Y. Cai, "Differential evolution enhanced with multiobjective sorting-based mutation operators," *IEEE Trans. Cybern.*, vol. 44, no. 12, pp. 2792–2805, Dec. 2014.

[37] G. Corriveau, R. Guilbault, A. Tahan, and R. Sabourin, "Review and study of genotypic diversity measures for real-coded representations," *IEEE Trans. Evol. Comput.*, vol. 16, no. 5, pp. 695–710, Oct. 2012.

[38] M. Epitropakis, D. Tasoulis, N. Pavlidis, V. Plagianakos, and M. Vrahatis, "Enhancing differential evolution utilizing proximity-based mutation operators," *IEEE Trans. Evol. Comput.*, vol. 15, no. 1, pp. 99–119, Feb. 2011.

[39] S. Mirjalili, S. M. Mirjalili, and A. Lewis, "Grey wolf optimizer," *Adv. Eng. Softw.*, vol. 69, pp. 46–61, Mar. 2014.

[40] S. Mirjalili, "The ant lion optimizer," *Adv. Eng. Softw.*, vol. 83, pp. 80–98, May 2015.

[41] J. J. Liang, A. K. Qin, P. N. Suganthan, and S. Baskar, "Comprehensive learning particle swarm optimizer for global optimization of multimodal functions," *IEEE Trans. Evol. Comput.*, vol. 10, no. 3, pp. 281–295, Jun. 2006.

[42] W. Gong, Z. Cai, and C. X. Ling, "DE/BBO: A hybrid differential evolution with biogeography-based optimization for global numerical optimization," *Soft Comput.*, vol. 15, no. 4, pp. 645–665, 2010.

[43] X. Chen, H. Tianfield, W. Du, and G. Liu, "Biogeography-based optimization with covariance matrix based migration," *Appl. Soft Comput.*, vol. 45, no. 3, pp. 71–85, Aug. 2016.

YUANZHE ZHAO received the B.S. degree in electrical engineering and automation and the Ph.D. degree in power system and automation from Southwest Jiaotong University, Chengdu, China, in 2009 and 2016, respectively.

He currently holds a postdoctoral position with the College of Transportation Engineering and the National Maglev Transportation Engineering Technology Research Center, Shanghai, China. His research interests include power quality analysis and control, harmonic analysis, and control of electrical drives.

LINJIE REN received the B.S. degree in industrial automation and the M.S. degree in control theory and control engineering from Lanzhou Jiaotong University, Lanzhou, China, in 2011 and 2017, respectively. He is currently pursuing the Ph.D. degree with Tongji University.

His current research interests include control with applications to mechatronic systems, and power quality analysis and control.

GUOBIN LIN received the B.S. degree in electric machine from Zhejiang University, Hangzhou, China, in 1986, and the M.S. degree in electrical engineering from Southwest Jiaotong University, Chengdu, China, in 1989.

He is currently a Professor and the Deputy Director of the National Maglev Transportation Engineering Technology Research Center, Tongji University, Shanghai, China. His research interests include maglev vehicle and linear drive research. Since 2014, he has been a member of the Steering Committee of International Maglev System and Linear Drive Conference.

ZHIMING LIAO received the B.S. degree in mechanical design and manufacturing from the Wuhan University of Hydraulic and Electrical Engineering, Wuhan, China, in 1995, and the M.S. degree in power electronics and electrical drives from Southwest Jiaotong University, Chengdu, China, in 2003. He is currently a Senior Engineer with the National Maglev Transportation Engineering Research and Development Center, Tongji University, Shanghai, China. His main research interests include linear motor design, motor control, and power supply system of maglev train.

SIMING LIU received the B.S. degree in communication engineering from Southwest Jiaotong University, Chengdu, China, in 2019. He is currently pursuing the master's degree in transportation engineering with Tongji University.

His current research interests include industrial ethernet, control over networks, and linear drive and communications in maglev and railway.